Supporting Information

Synergistic Effects of Li_3InCl_6/VGCF Composite Coating on the Electrochemical Performance of Single-Crystalline $LiNi_{0.6}Co_{0.1}Mn_{0.3}O_2$ Cathodes for All-Solid-State Lithium Batteries

Yu-Han Tsai,[a] Celastin Bebina Thairiyarayar,[a] Cheng-Wei Kao,[b] Jeng-Kuei Chang,[c] Soorathep Kheawhom,[d] Qunjie Xu[e,f] and Wei-Ren Liu[a,d,*]

[a] Department of Chemical Engineering, R&D Center for Membrane Technology, Chung Yuan Christian University, Taoyuan City, 320314, Taiwan

[b] National Synchrotron Radiation Research Center, Hsinchu, 30076, Taiwan

[c] Department of Materials Science and Engineering, National Yang Ming Chiao Tung University, Hsinchu 30010, Taiwan

[d] Department of Chemical Engineering, Faculty of Engineering, Chulalongkorn University, Bangkok, 10330, Thailand

[e] Shanghai Key Laboratory of Materials Protection and Advanced Materials in Electric Power, Shanghai Engineering Research Center of Energy-Saving in Heat Exchange Systems, Shanghai University of Electric Power, Shanghai 200090, China

[f] Shanghai Institute of Pollution Control and Ecological Security, Shanghai 200092, China

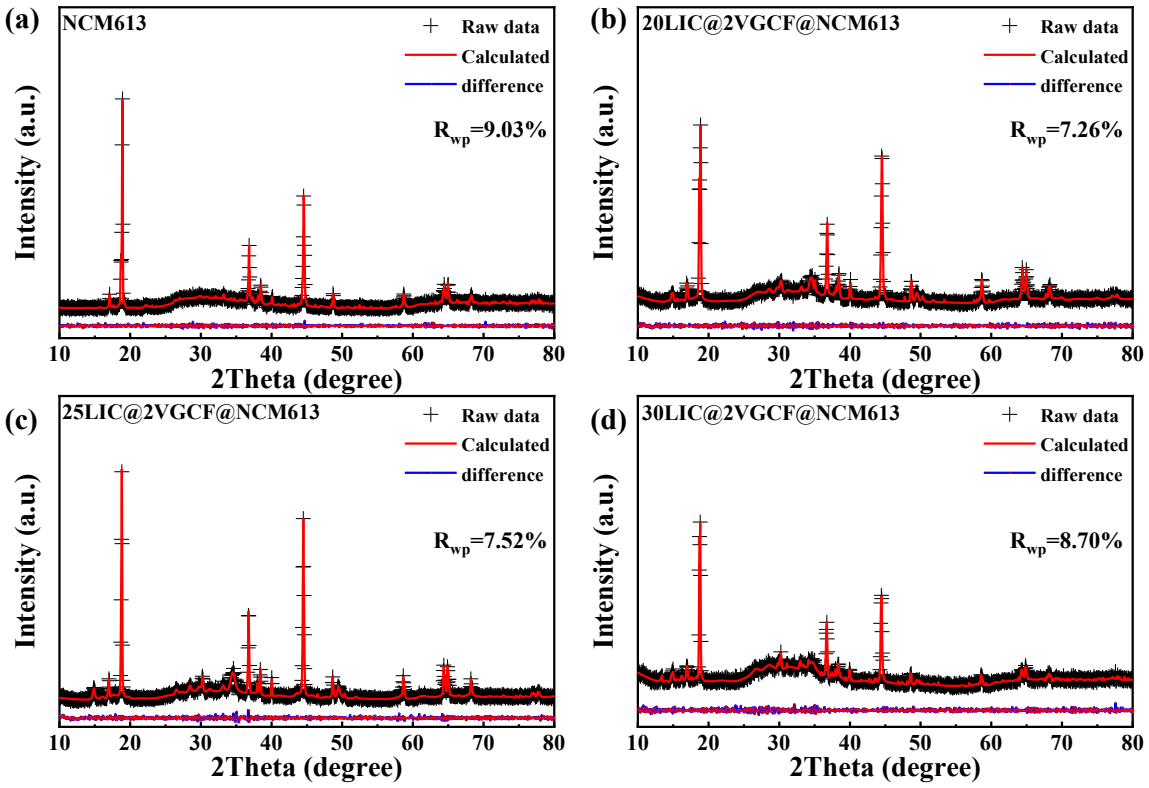

Figure S1. XRD Rietveld refinement profiles of SC-NCM613 cathode materials with varying Li_3InCl_6 coating ratios using TOPAS software: (a) SC-NCM613; (b) 20LIC@2VGCF@NCM613; (c) 25LIC@2VGCF@NCM613; (d) 30LIC@2VGCF@NCM613.

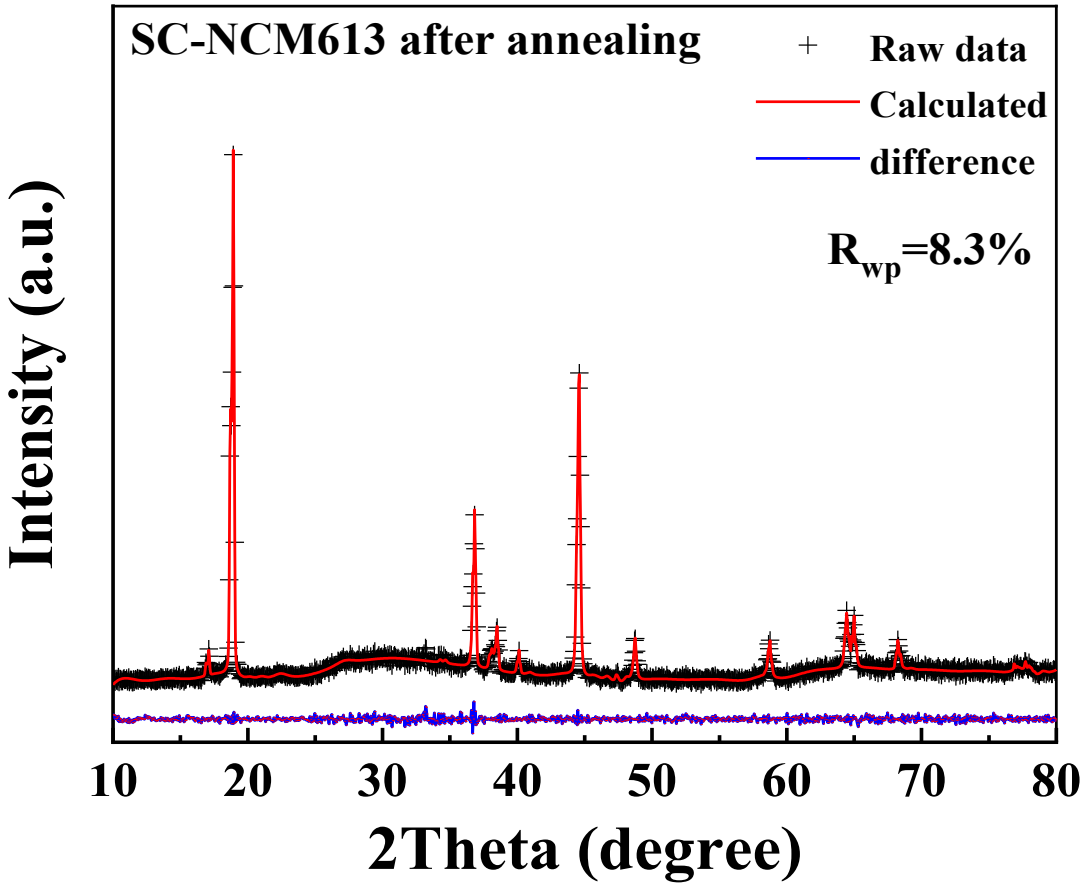

Figure S2. XRD Rietveld refinement profiles of heat-treated SC-NCM613 cathode material using TOPAS software.

Table S1. Lattice parameters of heat-treated single-crystalline NCM613 determined by Rietveld refinement.

Samples	*a* (Å)	*c* (Å)	*c*/*a*	Cell Volume(Å^3)	R_{wp} (%)	$I_{(003)}/I_{(104)}$
NCM613 After annealing	2.868(7)	14.2070(6)	4.952	101.25(6)	8.302	1.6746

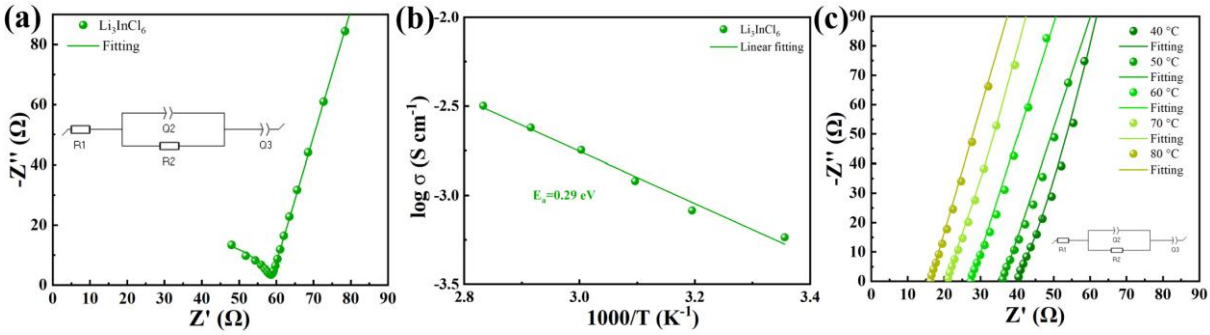

Figure S3. (a) Nyquist plots at RT, (b) Arrhenius plot and their corresponding Nyquist plot (c) at different temperatures of Li_3InCl_6 (Inset: Equivalent circuit).

Table S2. Ionic conductivities and their resistance values of Li_3InCl_6.

Li_3InCl_6	**R_1 (Ω)**	**R_2 (Ω)**	**$R_{tot}=(R_1+R_2)$ (Ω)**	**L (cm)**	**Ionic conductivity ($\times10^{-3}$ S cm^{-1})**
25 °C	25.76	32.51	58.27	0.062	1.355
40 °C	37.57	2.742	40.312	0.062	1.958
50 °C	30.12	5.793	35.913	0.062	2.198
60 °C	25.69	1.871	27.561	0.062	2.864
70°C	21.15	2.986	24.136	0.062	3.271
80 °C	15.53	0.63	16.16	0.062	4.885

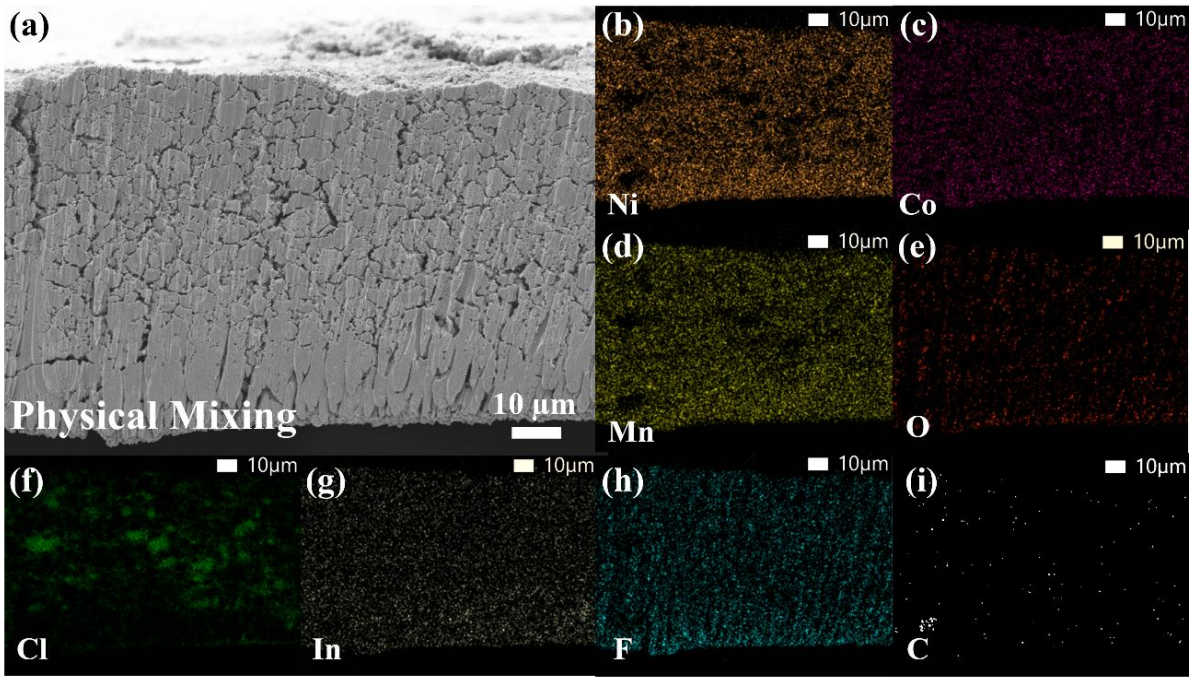

Figure S4. Composite cathode prepared by physical mixing: (a) scanning electron microscopy (SEM) image; (b–i) energy-dispersive X-ray spectroscopy (EDS) elemental maps for (b) Ni, (c) Co, (d) Mn, (e) O, (f) Cl, (g) In, (h) F, and (i) C.

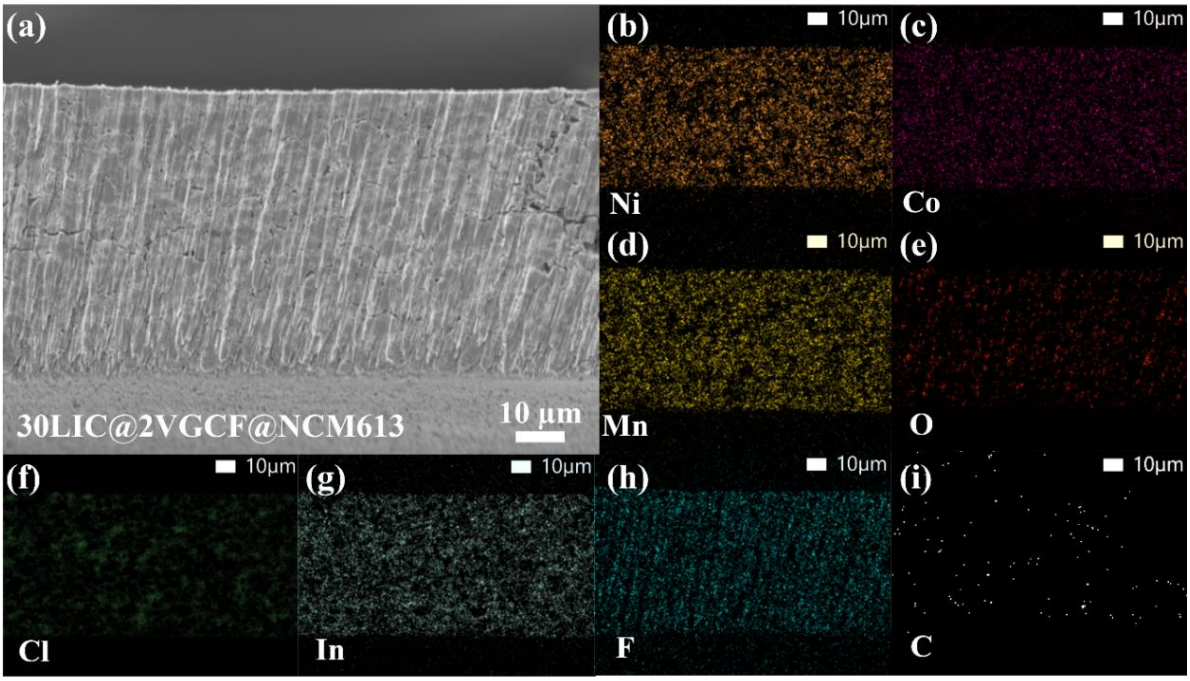

Figure S5. 30LIC@2VGCF@NCM613-prepared composite cathode: (a) scanning electron microscopy (SEM) image; (b–i) energy-dispersive X-ray spectroscopy (EDS) elemental maps of (b) Ni, (c) Co, (d) Mn, (e) O, (f) Cl, (g) In, (h) F, and (i) C.

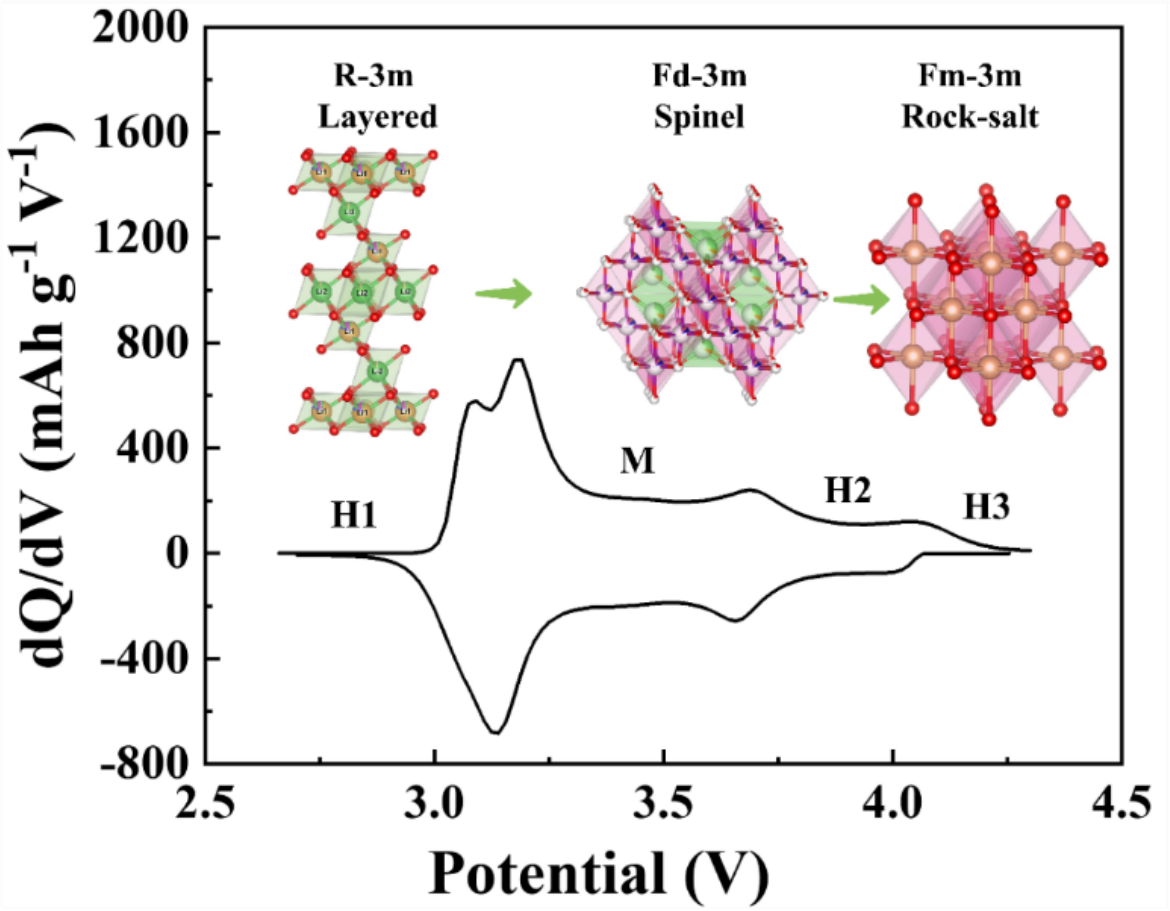

Figure S6. Schematic illustration of the phase-transition and corresponding microstructural evolution of the SC-NCM613 ($LiNi_{0.6}Co_{0.1}Mn_{0.3}O_2$) composite cathode during the first charge–discharge cycle.

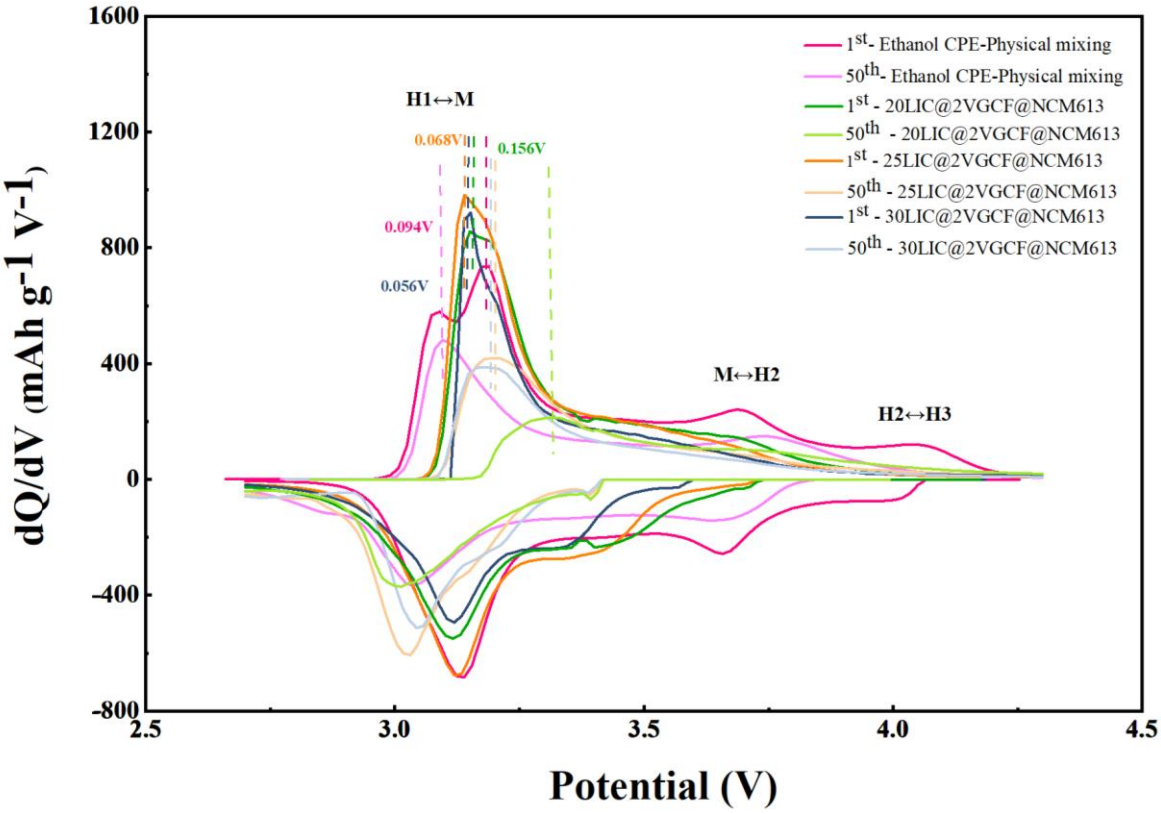

Figure S7. Comparison of derivative capacity (dQ/dV) plots of SC-NCM613 (Ethanol CPE-Physical mixing) and coated with varying Li_3InCl_6 ratios during 1st and 50th cycles.

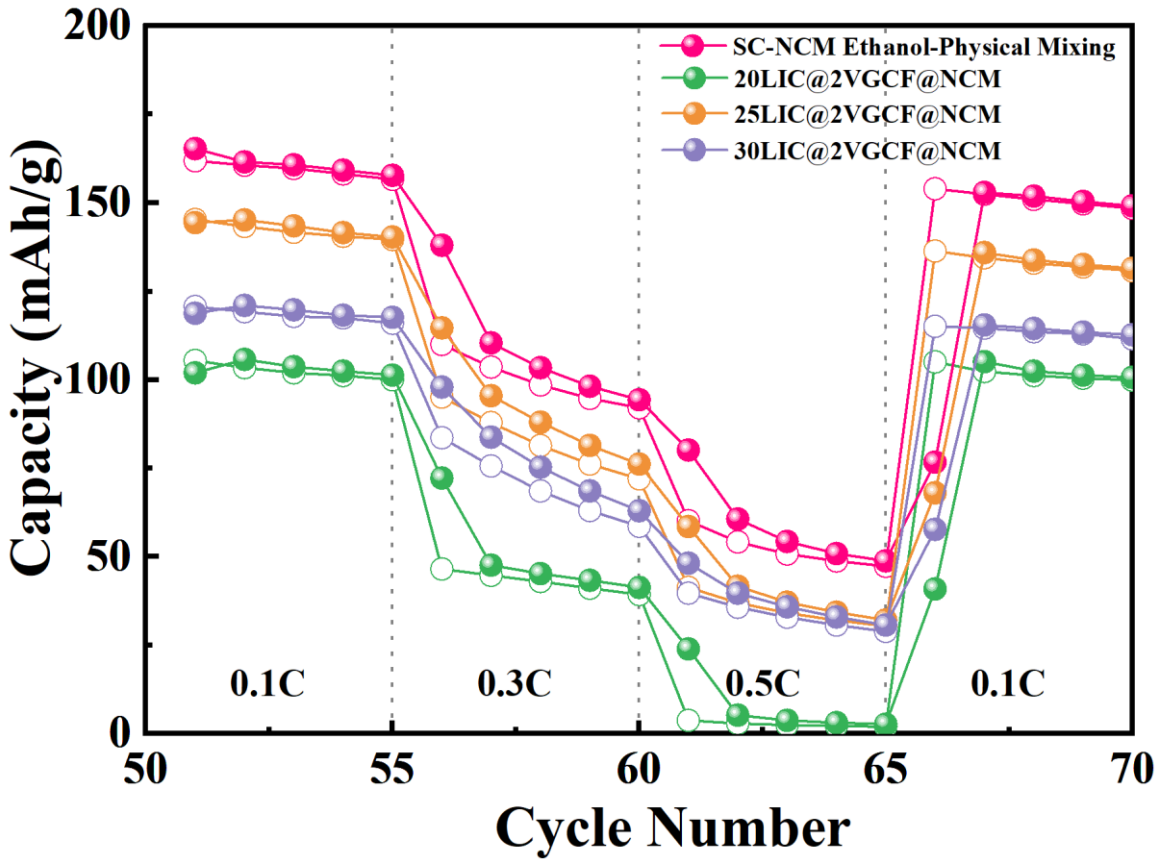

Figure S8. Rate capability tests of SC-NCM613 and coated with varying Li_3InCl_6 ratios after 50 cycles.

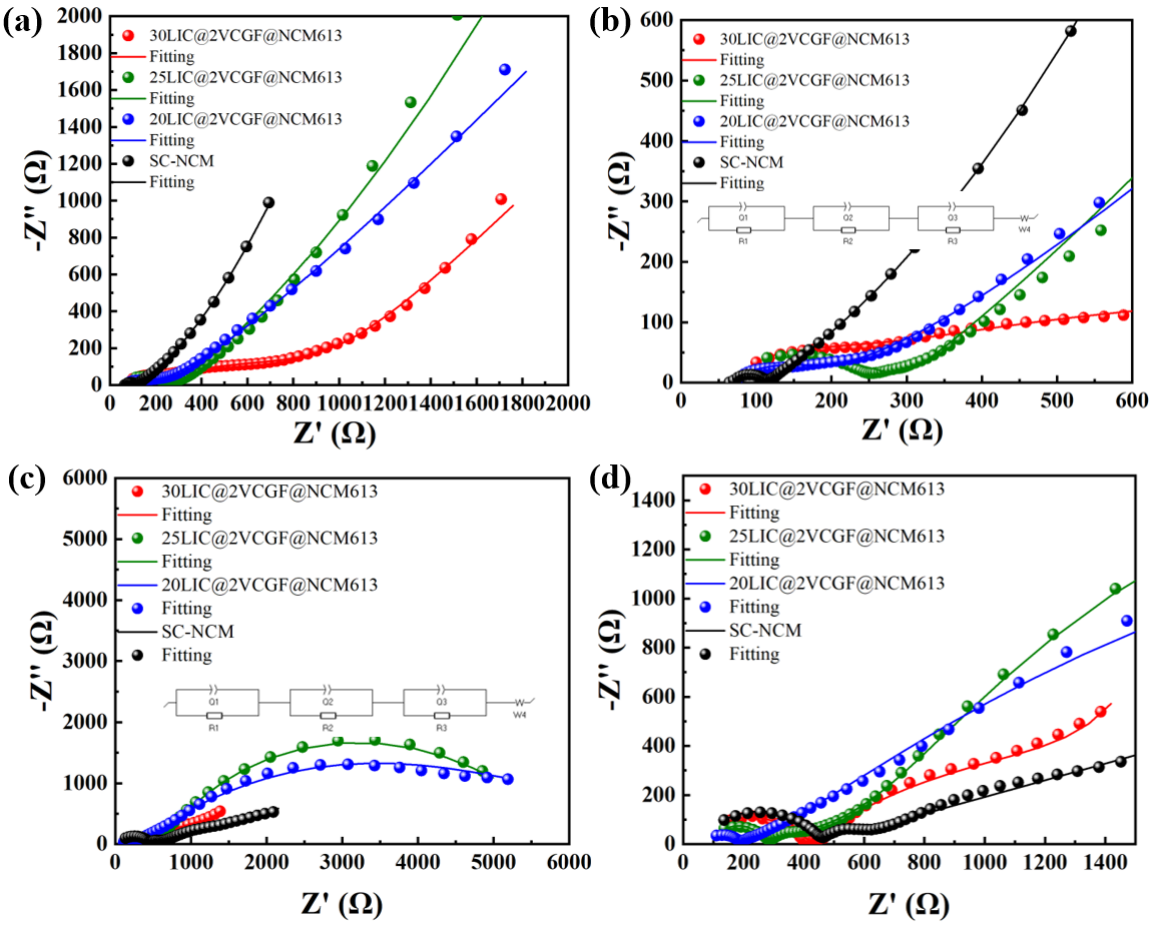

Figure S9. Nyquist plots of before (a) - (b) enlarged view and after (c) - (d) enlarged view of SC-NCM613 coated with varying Li_3InCl_6 ratios at 10 cycles (Inset: Equivalent circuit).

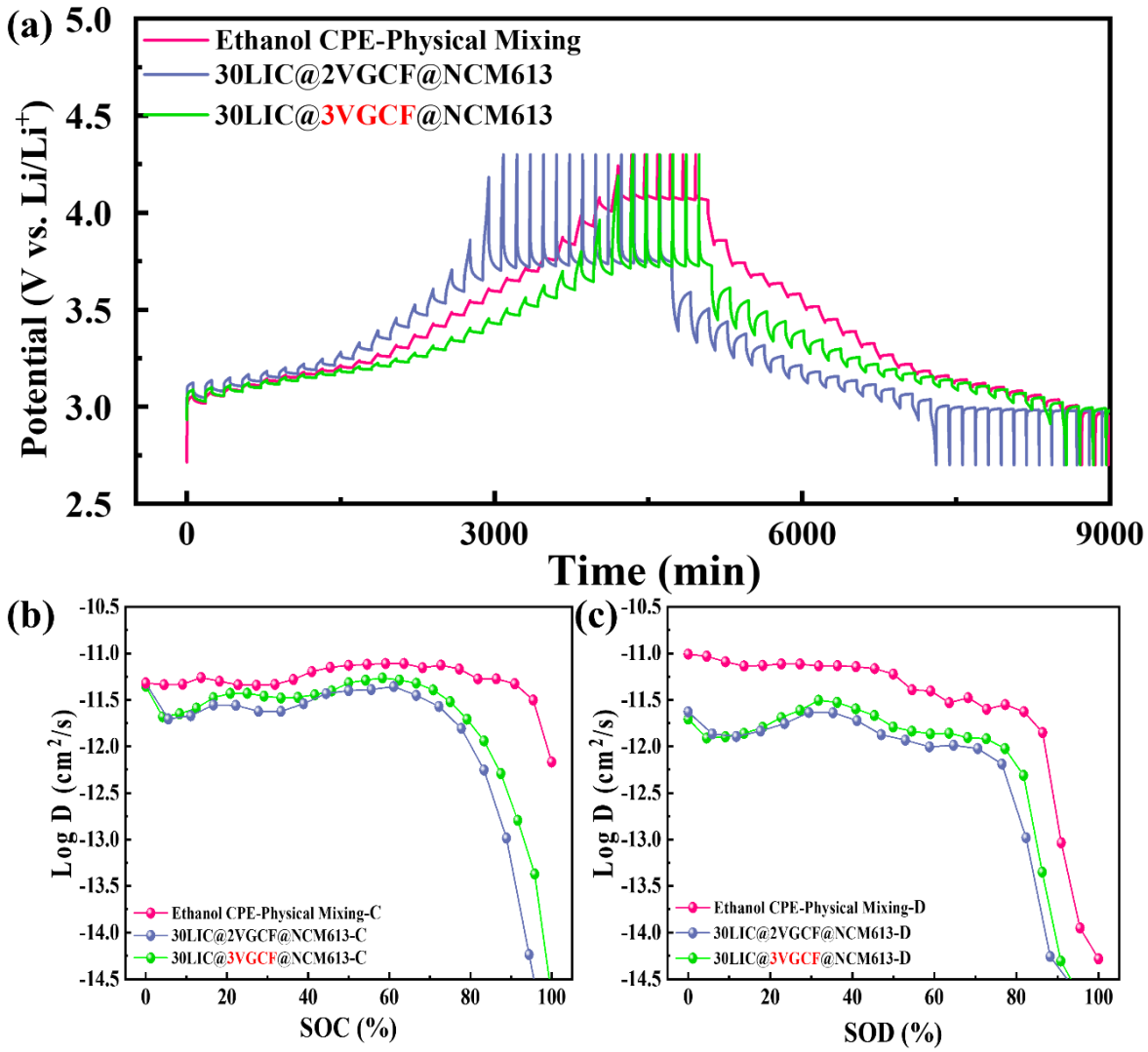

Figure S10. (a) GITT test results during the first cycle for the physically mixed SC-NCM613 composite cathode material, and the NCM@2VGCF@30LIC and NCM@3VGCF@30LIC cathode materials; (b) the corresponding lithium-ion diffusion coefficients (D_{Li^+}) during the charging process; (c) the corresponding lithium-ion diffusion coefficients (D_{Li^+}) during the discharging process.

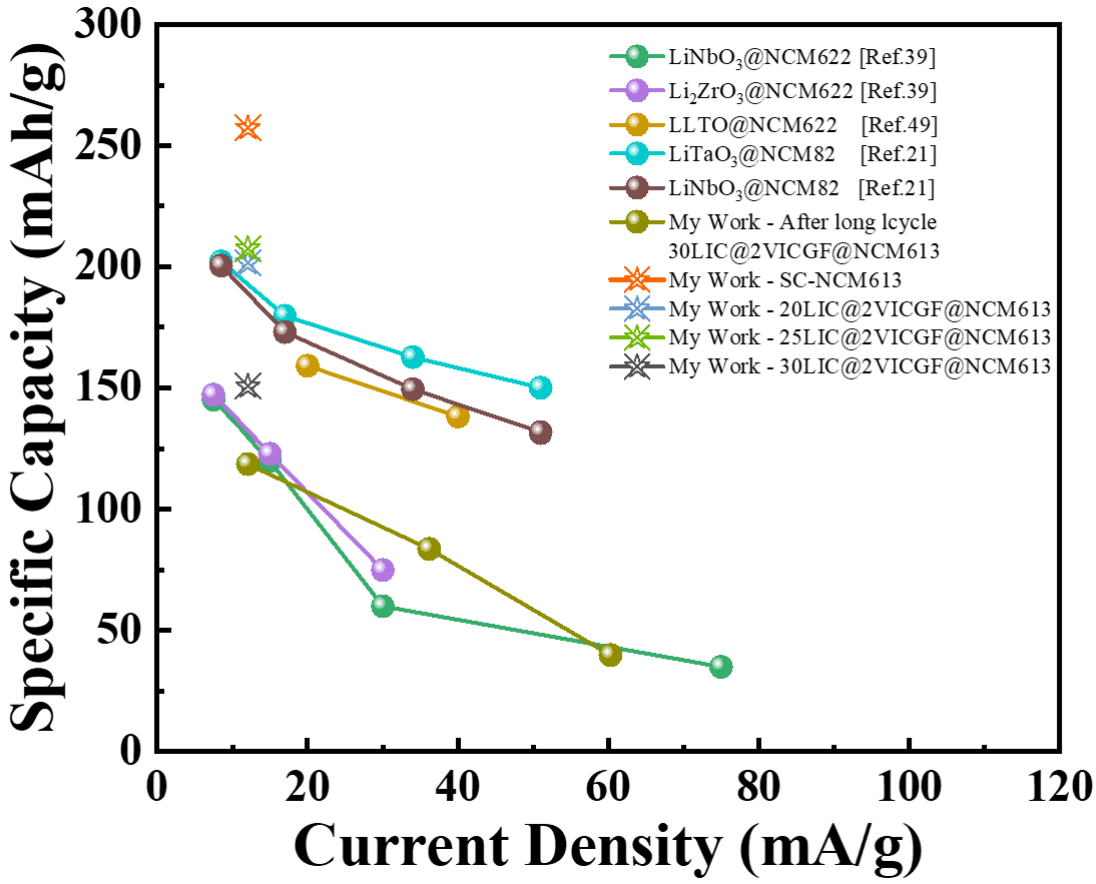

Figure S11. Comparative study of specific capacities between literature reports and present results.